Am J Clin Exp Urol 2025;13(1):20-32
www.ajceu.us /ISSN:2330-1910/AJCEU0160580

Original Article

2'-Hydroxyflavanone inhibits bladder cancer cell proliferation and angiogenesis via regulating miR-99a-5p/mTOR signaling

Tianyu Qi[1*], Fei He[1*], Shiqi Wu[1], Qi Wang[1], Jun Huang[2], Ruijie Dai[1], Zhangdong Jiang[1], Mingguo Zhou[1], Dalin He[1], Kaijie Wu[1]

[1]Department of Urology, The First Affiliated Hospital of Xi'an Jiaotong University, Xi'an 710061, Shaanxi, China; [2]Department of Urology, The Second Xiangya Hospital of Central South University, Changsha 410011, Hunan, China. [*]Equal contributors.

Received September 17, 2024; Accepted January 7, 2025; Epub February 15, 2025; Published February 28, 2025

Abstract: Objectives: 2'-Hydroxyflavanone (2HF) has been recognized for its antitumor potential in recent years. In the past decade, the role of miRNAs in tumors has been gradually explored. Since natural compounds may regulate miRNA networks, our objective is to investigate the potential effects and mechanisms of 2HF in the treatment of bladder cancer (BCa) by targeting miRNAs. Methods: Cell viability, tube formation, Transwell, western blotting and colony formation assays were used to evaluate the effects of 2HF on the viability and angiogenesis of BCa cells. The expression of miR-99a-5p and mTOR was detected via RT-qPCR and western blotting. A subcutaneous xenograft animal experiment was used to evaluate the tumor inhibition of 2HF in vivo. The binding of miR-99a-5p to mTOR was demonstrated via dual-luciferase reporting and RNA pull-down assays. Results: 2HF inhibited the cell viability, angiogenesis, protein expression of VEGFa and Ki67 in T24 and 253J cells and protein expression of CD31 in HUVEC cells. Also, 2HF induced the upregulation of miR-99a-5p but the downregulation of mTOR expression. Additionally, the inhibitory effect of 2HF on tumor cells can be effectively rescued by silencing miR-99a-5p or overexpressing mTOR in vitro. Moreover, 2HF inhibited tumor growth in nude mice, in which it upregulated miR-99a-5p but suppressed mTOR expression in xenograft tissues. Mechanistically, miR-99a-5p can directly target the mRNA of mTOR by binding to its 3' untranslated region (3'-UTR) and then inhibiting the expression of mTOR. Conclusions: 2HF inhibited BCa cell proliferation and angiogenesis by regulating the miR-99a-5p/mTOR/VEGFa axis, which may provide a novel treatment strategy and molecular mechanism for BCa treatment.

Keywords: 2'-Hydroxyflavanone, natural flavonoids, bladder cancer, angiogenesis, miR-99a, mTOR

Introduction

In 2022, more than 610,000 cases of bladder cancer (BCa) were diagnosed and more than 220,000 deaths were caused worldwide [1-3]. Urothelial carcinoma accounts for approximately 90% of BCa cases and strongly threatens the survival of patients [4, 5]. Radical cystectomy is recommended as the standard treatment for muscle-invasive bladder cancer [6]. However, many patients still experience cancer progression and develop treatment resistance [7-9]. Therefore, there is an urgent clinical need to develop more effective drugs and clinical strategies.

In recent decades, researchers have sought plant extracts with high biological activity from nature [10-13]. Flavonoids are a group of natural substances with variable phenolic structures, which have effects on a wide variety of biological processes, including the regulation of inflammatory responses, antioxidative and antitumor [14, 15]. The natural flavonoid 2'-hydroxyflavanone (2HF) is commonly extracted from oranges, lianas, and *Hovenia dulcis*, and has been widely recognized for its potent antitumor activity in kidney, pancreatic, prostate, and colon cancers [16-19]. Previously, our studies have revealed that 2'-hydroxyflavanone has good tumor suppressive effects on urinary tumors [20, 21].

MicroRNAs (miRNAs) are a class of single-stranded noncoding RNAs that play specific

https://doi.org/10.62347/CBAO9374

roles in BCa tumorigenesis and progression [22]. In recent years, many researchers have reported that some natural drugs may interact with miRNAs to jointly regulate some biological characteristics in vivo [23, 24]. MiR-99a-5p is well known as a tumor suppressor. In BCa, miR-99a-5p has been shown to inhibit cell proliferation or epithelial-mesenchymal transition (EMT) and induce cell senescence and apoptosis [25, 26]. Therefore, some researchers have proposed that miR-99a can be used as a potential biomarker in BCa diagnosis and treatment [27, 28].

In this study, we demonstrated that 2HF inhibited cell viability, vascular endothelial cell tube formation and recruitment in a dose-dependent manner in two BCa cell lines (T24 and 253J). Additionally, we found that 2HF regulated miR-99a-5p expression, and then inhibited mTOR and its downstream pathways by directly binding to the mTOR 3'UTR, thereby inhibiting BCa cell proliferation and angiogenesis.

Materials and methods

Cell culture, drug treatment and culture medium collection

Human BCa cell lines, T24 and 253J, were obtained from the Chinese Academy of Sciences Cell Bank of Type Culture Collection (CBTCCCAS, Shanghai, China). The cells were grown in standard medium containing 10% fetal bovine serum (FBS) at 37°C in a humidified environment with 5% CO_2. 2HF (99% pure, for research use) was purchased from Sigma-Aldrich (Germany) and dissolved in 100% dimethylsulfoxide (DMSO; Corning Cellgro; Manassas, VA) at a stock concentration of 100 mM. The stock solution was subsequently diluted in PBS (pH 7.2) to obtain a working solution of 2HF (0-60 μM). The vehicle control was 0.2% DMSO. The cells were treated with various concentrations of 2HF in 1% FBS for 48 h at 37°C with 5% CO2. BCa cells (5×10^5) were seeded into 60 mm dishes with 10% FBS medium and then treated with 2HF at final concentrations of 0, 20, 40, 60 μM or 20 μM miRNA. After 12 h, the cells were washed with serum-free medium (SFM) and then cultured with 5 mL of SFM for 24 h. The supernatants of T24 and 253J were collected as culture media (CMs) and centrifuged to remove debris.

Plasmids and cell transfection

The cells were transfected with the pcDNA3.1 mTOR overexpression plasmid from GenePharma (Shanghai, China) and a matched negative control (NC). The miR-99a-5p mimics, NC mimic, miR-99a-5p inhibitor, and NC inhibitor were purchased from RiboBio (Guangzhou, China). Stably transfected cells were screened in medium containing 5 μg/mL puromycin, and puromycin-resistant cell clones were removed after 14 days.

Cell viability assay and colony formation assay

BCa cells were seeded in 96-well plates in advance at 2×10^3 cells per well, and after overnight stabilization, they were treated with various concentrations of 2HF (0-60 μM) for 48 h. The medium was removed and replaced with 200 μL of MTT (Sigma-Aldrich; Merck KGaA) in 200 μL, after which the mixture was incubated for 4 h under the normal culture conditions as described above. The medium was completely removed, and 200 μL of DMSO was added to the wells, which were subsequently vortexed well for 10 min. Optical density at 490 nm was measured by an automatic microplate reader (Bio-Tek Instruments, Winooski, USA) in 8 replicates.

For the long-term colony formation assay, medium-log phase cultured T24 and 253J cells were plated onto 24-well tissue culture plates at 1000 cells per well for 48 h and treated with different concentrations of 2HF for 2 weeks. Then, the plates were washed with phosphate-buffered saline (PBS), fixed with 4% paraformaldehyde and stained with crystal violet solution for 15 min. The number of colonies in five random fields was counted via microscopy.

In vitro HUVEC recruitment assay and tube formation assay

HUVECs were seeded in Transwell inserts at a density of 5×10^4 cells per well, and the same number of BCa cells with/without 2HF treatment for 24 h were seeded in the lower chamber. After coculture, the transwell inserts were gently rinsed, soaked in 4% paraformaldehyde for 15 min, and then transferred to 0.1% crystal violet for 20 min. Under an inverted optical microscope (× 100), three fields of view and cell numbers were randomly collected. HUVECs were suspended in CM and then added to

24-well plates coated with Matrigel for tube formation. Pictures were taken after 6 h.

Western blotting

BCa cell proteins were collected in RIPA buffer containing proteinase inhibitors (1% inhibitor cocktail and 1 mM PMSF) (Roche Applied Science, Germany). A BCA protein assay kit and loading buffer (Beyotime) were used for concentration determination and protein denaturation, respectively. Proteins were separated on 10% SDS-PAGE gels and transferred to PVDF membranes at 110 V for 2 h. After blocking with 5% nonfat milk, the membranes were incubated with primary antibodies (VEGFa, Ki67, mTOR, p-mTOR and CD31 from Cell Signaling Technology, USA and GAPDH from Proteintech, China) at 4°C overnight. Next, the membranes were washed with TBST buffer 3 times and incubated with peroxidase-conjugated secondary antibodies for 1 h at room temperature. The membranes were visualized with an enhanced chemiluminescence (ECL) detection system (Bio-Rad, USA). ImageJ software was used for relative protein densitometric analysis.

RT-qPCR

Total RNA from cells was extracted via TRIzol (Invitrogen), and reverse transcription was performed via the TransScript First-Strand cDNA Synthesis SuperMix Kit (TransGen Biotech, Beijing, China) according to the manufacturer's recommendations. 18S was used to normalize the RNA levels via the 2-ΔΔCt method. The sequences of the primers used for RT-qPCR were as follows: miR-99a-F: 5'-CAACATACCCGTACTACAGGA-3'; miR-99a-R: 5'-TTCATCTACCCGTTCATACCC-3'; mTOR-F: 5'-TACAGAGAAACTGGCATCACT-3'; and mTOR-R: 5'-CAACCCCTC CCCAGAACCA-3'.

Dual-luciferase reporter assay

In accordance with the protocol, site-directed mutagenesis and sequencing of DNA fragments were performed via the QuikChange Lightning Directed Mutagenesis Kit (Agilent Technologies). The designed oligonucleotide strand was amplified, subcloned, and inserted into the pGL4-Basic vector (GenePharma, Shanghai, China) during annealing with T4 DNA Ligase (Roche). T24 and 253J cells were seeded in 24-well plates at a density of 1×10^4 cells per well for 24 h before transfection. The cells were transfected with the indicated luciferase reporter plasmids, miRNA mimics, and internal control luciferase reporter vectors (pRL-TK) (GenePharma, Shanghai, China) via Lipofectamine 3000 (Thermo Fisher Scientific, MA, USA) following the manufacturer's protocol. Luciferase and Renilla signals were measured 48 h after transfection via a Dual-Luciferase Reporter Assay Kit (GenePharma, Shanghai, China). Luciferase activity was normalized to the corresponding Renilla luciferase values for the calculation of fold changes.

RNA pull-down

BCa cells were seeded at 5×10^5 cells/well in six-well plates with complete DMEM overnight. The medium containing biotinylated miRNA (Roche, USA) and the transfection reagent was replaced for 24 h, followed by retransfection for 24 h. After that, the prepared streptavidin magnetic beads were mixed with 300 μL of cell lysate thoroughly for 4 h to bind to the target biotin-RNAs. Total RNA was extracted from the resuspended beads (TRIzol method), followed by cDNA preparation and RT-qPCR following the SYBR Green protocol.

Subcutaneous xenograft experiments

Male BALB/c nude mice (4 weeks old) were purchased from the Experimental Animal Center of Xi'an Jiaotong University and were housed under pathogen-free conditions in the Animal Laboratory of Xi'an Jiaotong University. The ambient temperature for feeding is maintained at 26°C with a relative humidity of 50%, and the environment follows a 12-hour light-dark cycle. Animal experiments were performed according to protocols approved by the Ethics Review Committee of Xi'an Jiaotong University. All of the mice were acclimatized to each other for 1 week. The mice were randomly grouped (n = 8 mice per group, the control group (corn oil 100 μL/day, gavage) and the 2HF group (50 mg/kg/day, gavage) via the random number method. Ea ch mouse model was established by injecting 2×10^6 T24 cells subcutaneously into the flanks of the mice, and we determined the tumor volume for each mouse every five days as $0.5 \times \text{length} \times \text{width}^2$. The mice were sacrificed after 4 weeks, and the tumor specimens were harvested for further experiments.

At the endpoint, the mice were euthanized via cervical dislocation, the tumor tissues were harvested, and the tumor weights were mea-

sured. Then, the tumor tissues were fixed in 10% buffered formalin for 48 h for immunohistochemistry (IHC). The remaining parts were washed with PBS and then frozen at -80°C for RT-qPCR measurement.

TCGA and GEO database analysis

The dataset GSE36121 containing publicly available mRNA-seq data was used, and no data availability statement was needed. Z score normalization was applied to all the data before further analysis. EdgeR was used to identify differentially expressed miRNAs between 16 BCa patients and 8 normal bladder donors. To ensure the accuracy of the sequencing data analysis, miRNAs with p values < 0.05 and fold changes ≥ 2 were considered significant DEGs and DECs. Visualization of the expression profile was performed via heatmaps.

Statistical analysis

SPSS 28.1 (IBM, SPSS, Chicago, IL, USA) and GraphPad Prism V9.3.1 (GraphPad Software, CA, USA) were used to analyze the results. One-way ANOVA or Student's t test was performed to evaluate the differences between the groups. The log-rank test was used to determine the significant differences between survival curves. Correlations between two groups were analyzed via Pearson's correlation coefficient analysis. A two-tailed $P < 0.05$ was considered statistically significant, and $P < 0.01$ was considered highly significant.

Results

2HF suppressed BCa cell viability and tumor-associated angiogenesis

To explore the effects of 2HF on the inhibition of BCa cell proliferation and angiogenesis, T24 and 253J cell lines were treated with different doses of 2HF before different cell function assays were performed. The results of MTT assay revealed that the viability of T24 and 253J cells was significantly inhibited by 2HF at concentrations above 20 μM at 48 h (**Figure 1A**, *P < 0.05, ***P < 0.001), however, 2HF did not exhibit a significant effect on the viability of SV-HUC-1 and HUVEC cells (Figure S1A, S1B). Moreover, the number of colonies formed was decreased in 2HF-treated T24 and 253J cells (**Figure 1B**). The IC50 value of T24 cells was 37.04 ± 4.28 μM at 48 h, and that of 253J cells was 41.61 ± 1.83 μM at 48 h. HUVEC tube formation and recruitment assays revealed that the number of tube formations (**Figure 1C** and **1D**, ***P < 0.001) and migrated HUVECs (**Figure 1E** and **1F**, *P < 0.05, **P < 0.01, ***P < 0.001) decreased following 2HF treatment. Finally, western blotting analysis confirmed that 2HF inhibited the expression of a proliferation-related protein, Ki67, and an angiogenesis-related protein, VEGFa, in T24 and 253J cells, meanwhile, 2HF inhibited the expression of CD31 protein in HUVEC cells (**Figure 1G**). These data confirmed that 2HF could inhibit BCa cell proliferation and angiogenesis in vitro.

2HF upregulated miR-99a-5p but inhibited mTOR expression in BCa cells

Next, we attempted to identify misregulated miRNA genes in BCa cells. Our previous studies revealed that the IFIT5 complex could degrade precursor miRNAs and downregulation of miR-99a-5p was crucial in BCa development [29, 30]. We first examined miR-99a-5p expression in normal tissues and BCa tissues from patients in the TCGA cohort. MiR-99a-5p was significantly downregulated in BCa tissues (Figure S2A, ***P < 0.001), whereas miR-99a-5p in cancer tissues was also significantly downregulated in the matched tissues (Figure S2B, *P < 0.05). By comparing miRNA expression in normal, peripheral cancer, and core cancer tissues, we also identified the miR-99a-5p as one of the most significant downregulated miRNAs in the BCa cohort (Figure S2C). Additionally, normal bladder epithelial SV-HUC-1 cells were compared with BCa cell lines (T24 and 253J). Indeed, we found that miR-99a-5p expression was lower but mTOR expression was higher in T24 and 253J cells than in SV-HUC-1 cells (**Figure 2A** and **2B**, ***P < 0.001). According to the RT-qPCR results, miR-99a-5p was upregulated after 2HF treatment in BCa cells in a dose-dependent manner (**Figure 2C**, *P < 0.05, ***P < 0.001). Moreover, p-MTOR and mTOR were inhibited by 2HF in a dose-dependent manner (**Figure 2D**). Our study confirmed that miR-99a-5p and mTOR were involved in the pharmacological action of 2HF in BCa treatment.

Silencing miR-99a-5p promotes BCa cell viability and tumor-associated angiogenesis

To further clarify the role of miR-99a-5p in 2HF pharmacological actions, T24 and 253J cells

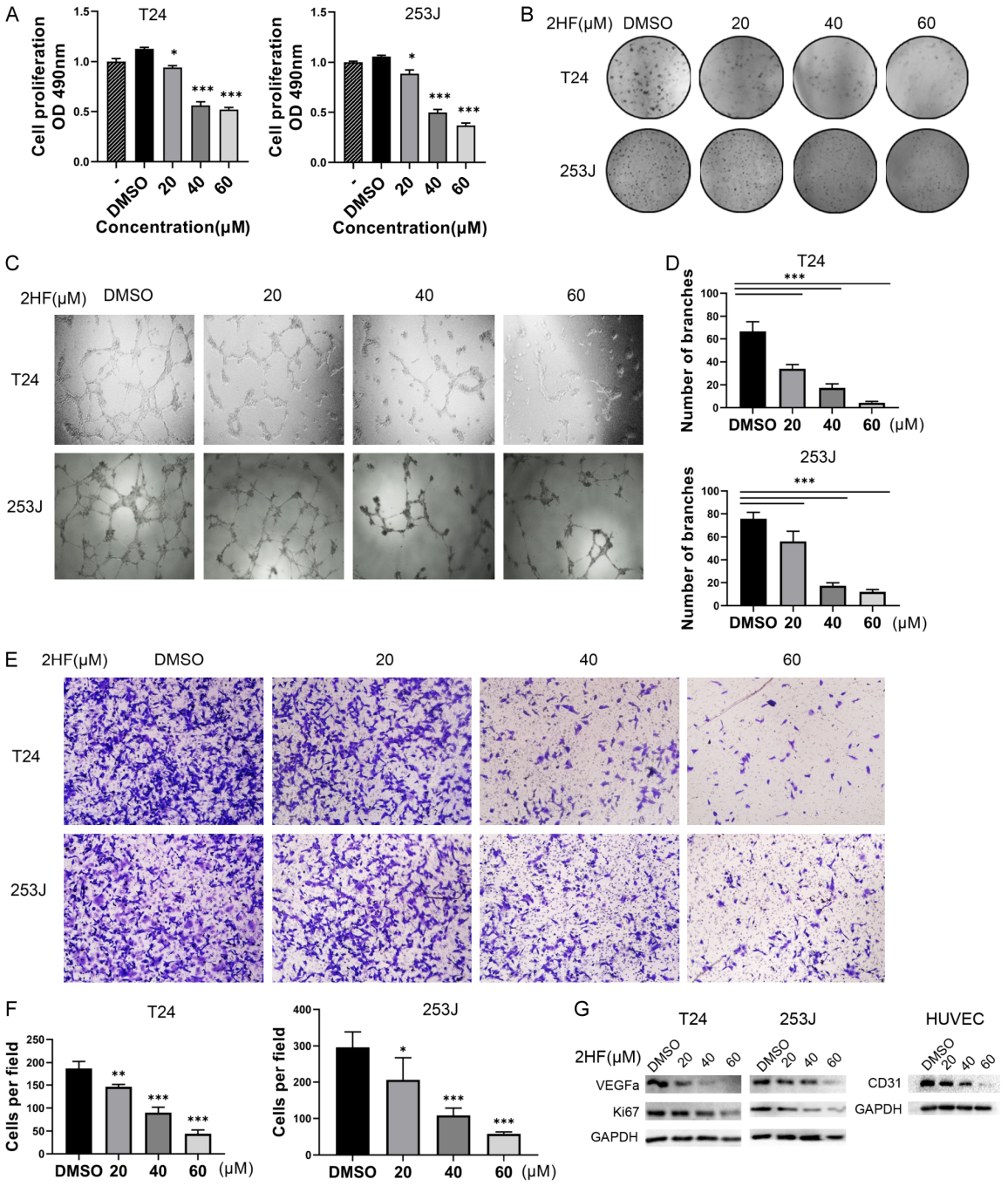

Figure 1. 2HF suppressed BCa proliferation and angiogenesis in vitro. A. MTT assay was used to measure the viability of T24 and 253J cells after 2HF treatment at 48 h. B. A colony formation assay was conducted in T24 and 253J cells after 2HF treatment. C. A tube formation assay was used to measure angiogenesis in T24 and 253J cells after 2HF treatment. D. Quantitative analysis of tube formation assay was shown. E. The HUVEC recruitment assay was used to measure the angiogenesis of T24 and 253J cells after 2HF treatment. F. Quantitative analysis of HUVEC recruitment assay was shown. G. Western blotting anaysis of Ki67 and VEGFa protein expression in T24 and 253J cells and CD31 protein expression in HUVEC cells after 2HF treatment. *P < 0.05, ***P < 0.001.

were transfected with miR-99a-5p single-chain inhibitors and controls supplemented with 2HF treatment. RT-qPCR revealed that miR-99a-5p expression was significantly downregulated in the miR-99a-5p inhibitor-transfected cells (**Figure 3A**, ***P < 0.001). Indeed, the miR-99a-

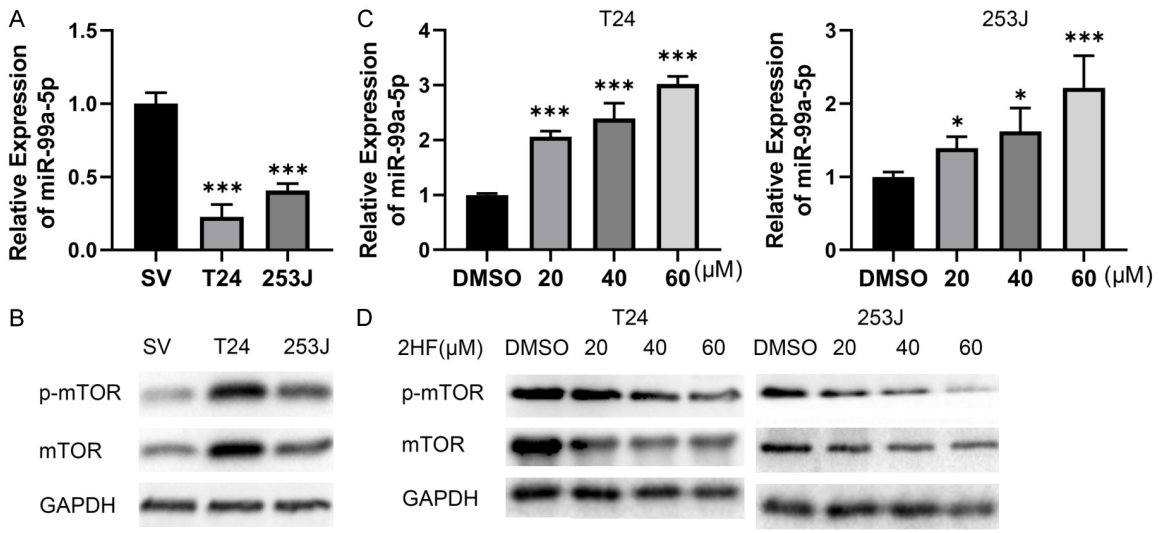

Figure 2. The expression of miR-99a-5p and mTOR in 2HF-treated BCa cells. A. RT-qPCR was used to detect the miR-99a-5p expression level in BCa and normal cell lines. B. Western blotting was used to detect the protein expression levels of mTOR and phosphorylated mTOR in BCa and normal cell lines. C, D. miR-99a-5p expression levels and mTOR and phosphorylated mTOR protein expression levels were detected in T24 and 253J cells treated with 2HF for 48 h. *P < 0.05, ***P < 0.001.

5p inhibitor could abolish the inhibitory effect of 2HF in cell growth, HUVEC tube formation, HUVEC cell recruitment and colony formation (**Figure 3B-G**, *P < 0.05, **P < 0.01, ***P < 0.001). Also, western blotting analysis revealed that miR-99a-5p blockade could rescue the expression of Ki67, VEGFa and CD31 inhibited by 2HF (**Figure 3H**). Our results revealed that miR-99a-5p mediated the tumor-inhibitory effect of 2HF in BCa tumor growth and angiogenesis.

miR-99a-5p directly regulates mTOR expression in BCa

Next, we further identified the regulatory role of miR-99a-5p in mTOR. Through the TargetScan and miRanda database, we identified the potential binding sequences of miR-99a-5p on mTOR-3'UTR, and then wild-type and mutant mTOR-3'UTR vectors were constructed (**Figure 4A**). T24 and 253J cells were co-transfected with the miR-99a-5p mimic and the mTOR 3'UTR WT or mTOR 3'UTR MUT vector, the luciferase assay results indicated that miR-99a-5p mimic could significantly suppress the luciferase activity of mTOR 3'UTR WT, but had no effect on mTOR 3'UTR MUT (**Figure 4B**, *P < 0.05). In addition, RNA pull-down was used to verify the direct binding of miR-99a-5p on mTOR mRNA, and the miR-99a-5p mimic effectively increased this binding in T24 and 253J cells (**Figure 4C**, *P < 0.05). Similarly, the expression of mTOR protein in these cells treated with the miR-99a-5p inhibitor was significantly enhanced, whereas the expression of mTOR in the miR-99a-5p mimic group was significantly suppressed (**Figure 4D**). Taken together, miR-99a-5p could directly regulate mTOR mRNA expression in BCa.

Overexpression of mTOR rescued the inhibition of tumor proliferation and angiogenesis by 2HF

Dysregulation of the mTOR pathway plays a complex role in tumor growth, so many scholars expect to enhance tumor therapeutic efficacy by targeting mTOR [31, 32]. Herein, the role of mTOR in 2HF-mediatied BCa treatment has been further explored. PcDNA3.1-mTOR and pcDNA3.1 vectors were used to transfect BCa cell lines and induce mTOR or p-mTOR overexpression (**Figure 5A**). 2HF and PBS were used to treat mTOR-overexpressing BCa cells before cell viability was determined. The results showed that mTOR overexpression could rescue the growth inhibition of tumor cells caused by 2HF (**Figure 5B**). Moreover, mTOR increased the ability of HUVECs tube formation in T24 and 253J cells and rescued the inhibitory effects of 2HF treatment (**Figure 5C** and **5D**, *P < 0.05,

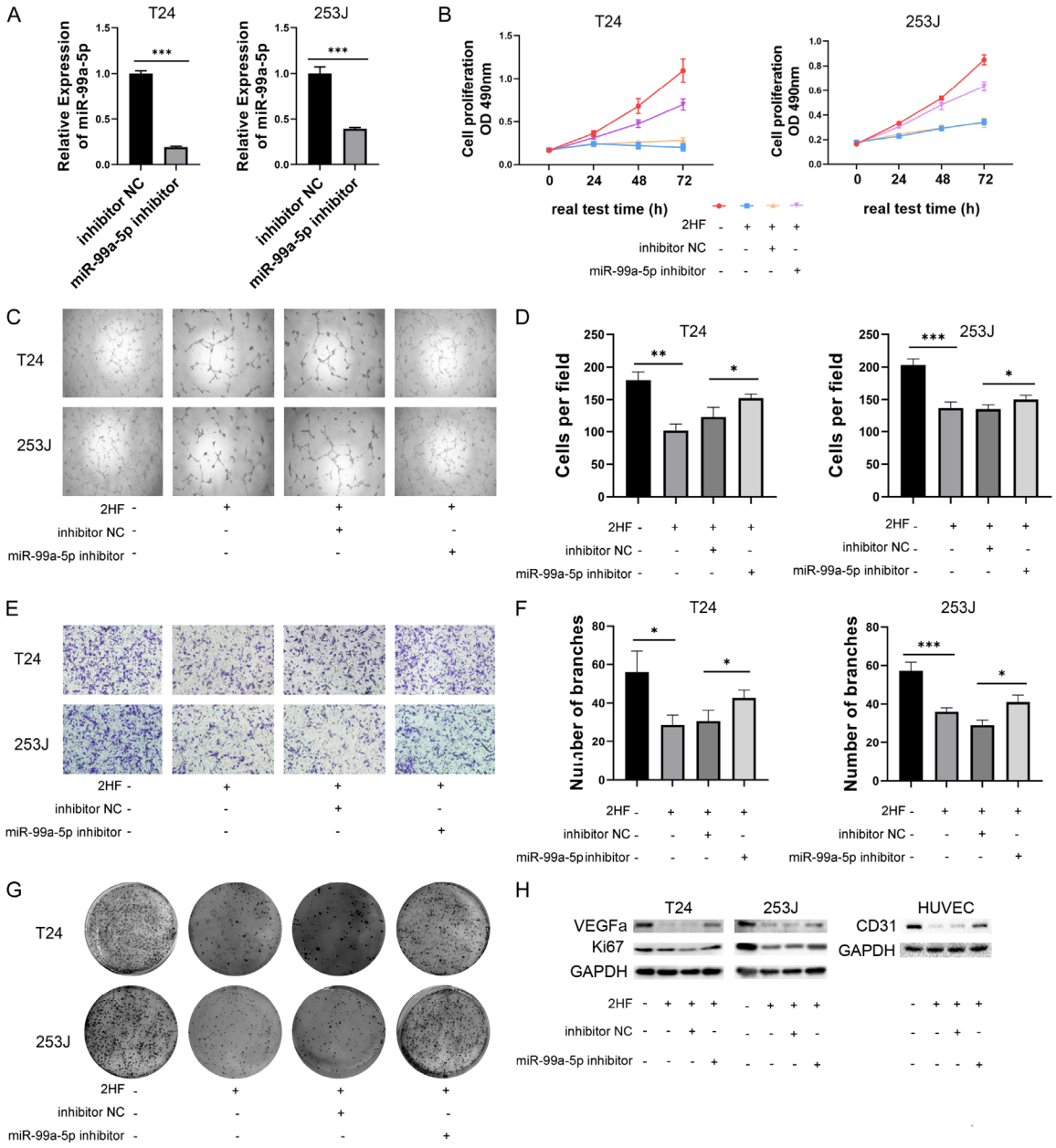

Figure 3. The blockade of miR-99a-5p abloshed the inhibitory effects of 2HF in BCa cell proliferation and angiogenesis in vitro. A. RT-qPCR was used to detect the miR-99a-5p level in T24 and 253J cells treated with the miR-99a-5p inhibitor. B. MTT assay was used to measure cell viability at 24, 48 and 72 h. C. A tube formation assay was used to measure angiogenesis in T24 and 253J cells. D. Quantitative analysis of tube formation assay was shown. E. The HUVEC recruitment assay was used to measure angiogenesis in T24 and 253J cells. F. Quantitative analysis of HUVEC recruitment assay was shown. G. A colony formation assay was conducted in T24 and 253J cells. H. Western blotting analysis of Ki67 and VEGFa expression levels in T24 and 253J cells, CD31 expression in HUVEC cells transfected with miR-99a-5p inhibitor combined with 2HF treatment. *P < 0.05, ***P < 0.001.

P < 0.01, ***P < 0.001). Similarly, HUVECs cell recruitment was also promoted by mTOR overexpression (Figure 5E** and **5F**, **P < 0.01, ***P < 0.001). Furthermore, we found that mTOR rescued BCa colony formation, Ki67, VEGFa and CD31 expression which was inhibited by 2HF treatment (**Figure 5G** and **5H**). These results confirmed that mTOR was essential for 2HF-mediated BCa proliferation and vascular growth inhibition.

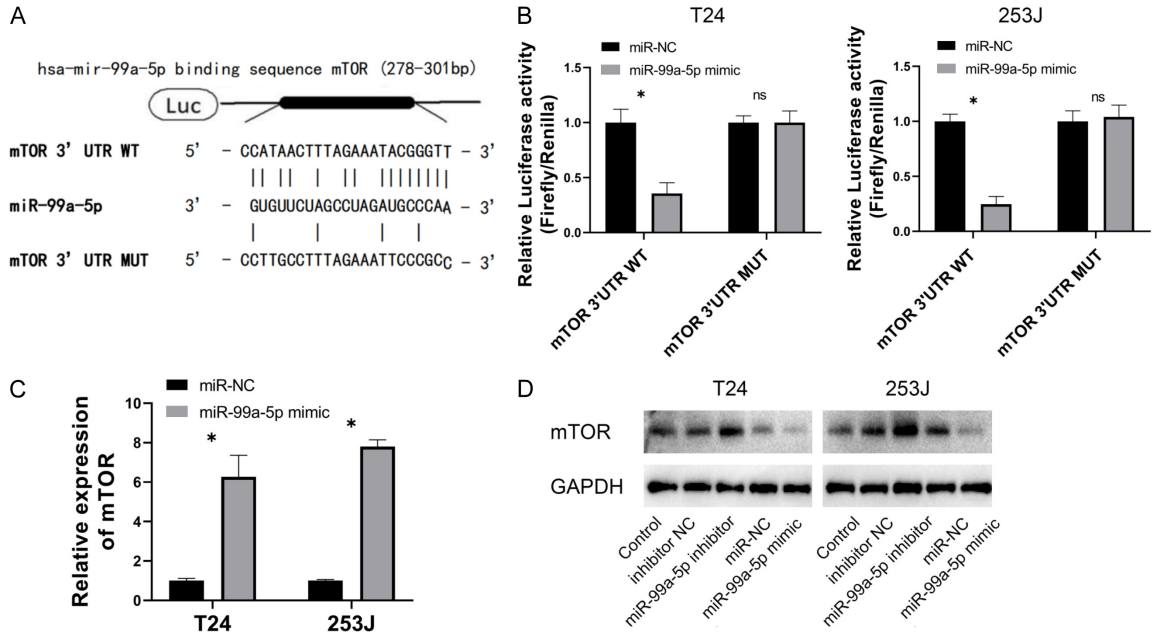

Figure 4. mTOR was a downstream target of miR-99a-5p in BCa cells. A. The results from TargetScan (http://www.targetscan.org) and miRanda (microRNA.org) showing the predicted miR-99a-5p binding sites in the 3'UTR of the mTOR mRNA. B. A luciferase reporter assay indicated that alterations in miR-99a-5p expression regulated the luciferase activity of the wild-type (WT), but not the mutant (MUT) mTOR 3'UTR plasmid. C. RNA pull-down assays were used to examine mTOR expression in T24 and 253J cells subjected to biomiR-99a-5p-mediated pull-down. D. mTOR protein expression in miR-99a-5p mimic- and inhibitor-transfected cells. *P < 0.05; ns, not significant.

2HF inhibits BCa growth and angiogenesis in vivo

Next, we further determined the anti-BCa role of 2HF in vivo. T24 cells were injected subcutaneously into nude mice gavaged with 2HF (100 mg/kg/day) or corn oil via intraperitoneal injection. The mice were weighed on Days 12, 15, 18, and 21 and the results revealed that the volume of xenograft tumors from the 2HF-treated group was significantly lower than that of the control group (**Figure 6A** and **6B**, **P < 0.01). The tumor tissue was collected and weighed 28 days after the xenografts were established. Consistently, the weight of xenograft tumors from the 2HF group were significantly lower than that of the control group (**Figure 6C**, **P < 0.01). The RT-qPCR results confirmed that 2HF upregulated miR-99a-5p expression in xenograft tumors (**Figure 6D**, **P < 0.01). Immunohistochemical staining (IHC) data indicated that 2HF treatment inhibited mTOR, Ki67, and VEGFa expression in xenograft tumor tissues (**Figure 6E**). In brief, we demonstrated that 2HF inhibited BCa tumor growth and angiogenesis in vivo.

Discussion

BCa is a heterogeneous disease characterized by extensive intratumor angiogenesis, which is a marker of BCa carcinogenesis and tumor progression. Among angiogenic inducers, VEGFa plays a significant role in angiogenesis both in vitro and in vivo [33].

mTOR has long been recognized as the mammalian target of rapamycin [34]. mTOR exists as a complex of two protein forms, mTORC1 and mTORC2 [35]. Researchers have reported that some upstream molecules, nutrients, and energy-sensing signals converge in the mTOR signaling pathway. PI3K/Akt is a key upstream signaling molecule of mTOR, and it has been shown that EGFR and HER2 can drive mTOR to activate cancer progression through PI3K/Akt in a variety of tumors [36, 37]. Similarly, the RAS-Raf-MEK-ERK pathway, which can be activated by growth factors [38], hormones [39], and cytokines [40], regulates mTOR. Mutations in RAS and its family proteins ultimately mediate abnormal activation of this pathway in many types of cancer. Our previous study confirmed that depletion of DAB2IP, a novel Ras-GTPase

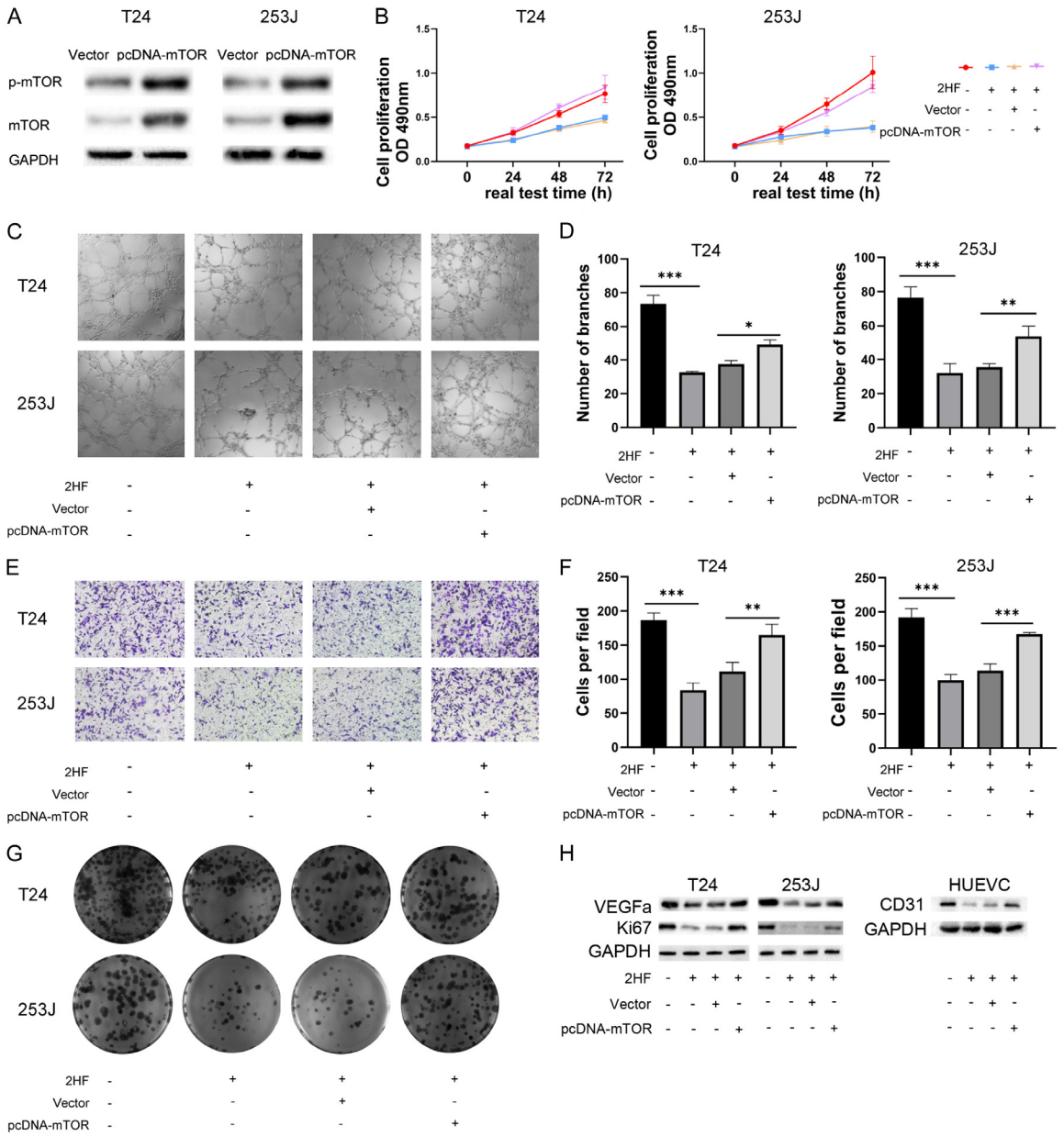

Figure 5. mTOR onverexpression abolished the inhibitory effect of 2HF in BCa cell proliferation and angiogenesis in vitro. A. mTOR protein expression was detected by western blotting in transfected cells. B. MTT assay was used to measure cell viability at 24, 48, and 72 h. C. HUVEC tube formation assay in T24 and 253J cells with mTOR overexpression and 2HF treatment. D. Quantitative analysis of HUVEC tube formation was shown. E. HUVEC recruitment assay in T24 and 253J cells with mTOR overexpression and 2HF treatment. F. Quantitative analysis of HUVEC recruitment was shown. G. A colony formation assay was conducted in T24 and 253J cells. H. Western blotting analysis of Ki67 and VEGFa protein levels in T24 and 253J cells, CD31 expression in HUVEC cells transfected with pcDNA-mTOR combined with 2HF treatment. *P < 0.05, **P < 0.01, ***P < 0.001.

activating protein, leads to the activation of ERK/RSK1 and the PI3K/mTOR pathway, which synergizes with the induction of hypoxia-inducible factor (HIF)-2α [41]. Therefore, targeting mTOR pathway provides a new therapeutic strategy for BCa treatment.

VEGFa as an inducer of HUVEC proliferation, migration, and invasion, meanwhile the proliferation of HUVECs was rapidly induced following incubation with the tumor culture supernatant. In this study, we demonstrated that 2HF significantly inhibited mTOR-mediated prolifera-

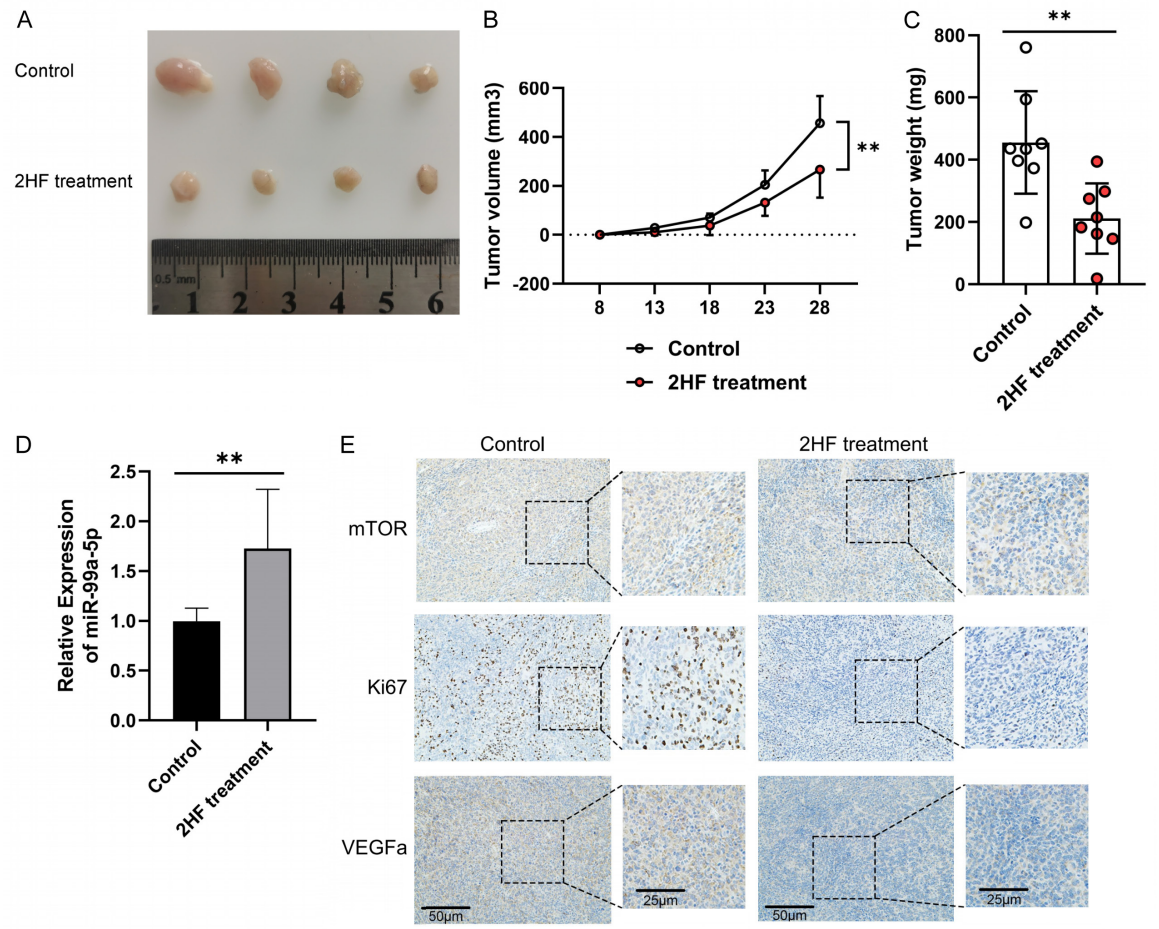

Figure 6. 2HF treatment attenuated the tumorigenicity and angiogenesis of BCa in vivo. A. Representative images of subcutaneous tumors derived from T24 cells after 2HF treatment. B. Tumor volume was measured every 5 days. C. After the mice were sacrificed at the end of the experiment, the wet weights of the tumors were compared. D. The expression of miR-99a-5p in xenograft tumors was detected via RT-qPCR. E. Immunohistochemistry was performed to detect the expression of mTOR, Ki67, and VEGFa in xenograft tumor tissues from different groups. Scale bar: 50 μm (left), 25 μm (right). **P < 0.01.

tion and angiogenesis in a dose-dependent manner, and also it could suppress the expression of Ki67 and VEGFa. Notably, 20 μM 2HF inhibited mTOR-mediated proliferation but had almost no effect on HUVEC viability. This finding suggested that 2HF may be a good natural tumor suppressor adjuvant.

Interestingly, through database screening and qPCR screening, we found that the inhibitory pharmacological effect of 2HF treatment in BCa was via the dysregulated miRNAs in tumor cells, in which miR-99a might play a critical role. MiR-99a has been identified as an inhibitor of BCa in several studies [25, 42-44]. Compared with that in other cancers [45], the function of miR-99a in BCa seems to be relatively stable, such as inhibition of cell proliferation, invasion and migration of BCa cells and induction of cell apoptosis. A recent study reported that miR-99a induced cell senescence in gemcitabine-resistant BCa cells [46]. In our study, we confirmed that 2HF could regulate miRNAs and show its pharmacological effects in BCa. First, the expression of miR-99a-5p was regulated in a 2HF dose-dependent manner. Second, miR-99a-5p directly regulated the activity of mTOR mRNA. Also, both miR-99a-5p and mTOR played roles in the inhibitory of 2HF in BCa tumor growth and angiogenesis. From this perspective, 2HF, as a naturally derived compound characterized by its abundant availability and cost-effectiveness, holds substantial medicinal potential. In the present study, it

demonstrated pronounced antitumor activity while exhibiting an overall low-to-negligible toxicity profile.

These findings suggest that 2HF may serve as a promising candidate for clinical applications, particularly in combination with chemotherapeutic agents to mitigate drug resistance, thereby contributing to the development of innovative cancer treatment strategies. Therefore, it is hypothesized that 2HF has the potential to serve as a promising adjuvant therapeutic agent in the future, however, this requires clinical validation and further investigation into the underlying mechanisms.

Acknowledgements

The authors acknowledge the contributions of all researchers to this article. This study was supported by the National Natural Science Foundation of China (NSFC 81202014 to KW), New-Star Young Scientists Program in Shaanxi Province (2017KJXX-35 to KW), Key Research and Development Program of Shaanxi Province (2022SF-307 to KW) and the Fundamental Research Funds for the Central Universities (to KW).

Disclosure of conflict of interest

None.

Address correspondence to: Kaijie Wu, Department of Urology, The First Affiliated Hospital of Xi'an Jiaotong University, No. 277 Yanta West Road, Xi'an 710061, Shaanxi, China. Tel: +86-29-8532-3945; Fax: +86-29-8532-3203; E-mail: kaijie_wu@163.com

References

[1] Bray F, Laversanne M, Sung H, Ferlay J, Siegel RL, Soerjomataram I and Jemal A. Global cancer statistics 2022: GLOBOCAN estimates of incidence and mortality worldwide for 36 cancers in 185 countries. CA Cancer J Clin 2024; 74: 229-263.

[2] Dobruch J, Daneshmand S, Fisch M, Lotan Y, Noon AP, Resnick MJ, Shariat SF, Zlotta AR and Boorjian SA. Gender and bladder cancer: a collaborative review of etiology, biology, and outcomes. Eur Urol 2016; 69: 300-310.

[3] Siegel RL, Miller KD, Fuchs HE and Jemal A. Cancer statistics, 2022. CA Cancer J Clin 2022; 72: 7-33.

[4] Tanaka MF and Sonpavde G. Diagnosis and management of urothelial carcinoma of the bladder. Postgrad Med 2011; 123: 43-55.

[5] Chamie K, Litwin MS, Bassett JC, Daskivich TJ, Lai J, Hanley JM, Konety BR and Saigal CS; Urologic Diseases in America Project. Recurrence of high-risk bladder cancer: a population-based analysis. Cancer 2013; 119: 3219-3227.

[6] Aminoltejari K and Black PC. Radical cystectomy: a review of techniques, developments and controversies. Transl Androl Urol 2020; 9: 3073-3081.

[7] Taylor JA 3rd and Kuchel GA. Bladder cancer in the elderly: clinical outcomes, basic mechanisms, and future research direction. Nat Clin Pract Urol 2009; 6: 135-144.

[8] Massari F, Santoni M, Ciccarese C, Brunelli M, Conti A, Santini D, Montironi R, Cascinu S and Tortora G. Emerging concepts on drug resistance in bladder cancer: implications for future strategies. Crit Rev Oncol Hematol 2015; 96: 81-90.

[9] Lopez-Beltran A, Cookson MS, Guercio BJ and Cheng L. Advances in diagnosis and treatment of bladder cancer. BMJ 2024; 384: e076743.

[10] Lee SJ, Choi JH, Son KH, Chang HW, Kang SS and Kim HP. Suppression of mouse lymphocyte proliferation in vitro by naturally-occurring biflavonoids. Life Sci 1995; 57: 551-558.

[11] Goldstein DH, Stolman A and Goldfarb AE. The influence of methyl chalcone of hesperidin on the toxicity of mapharsen in rabbits. Science 1943; 98: 245-246.

[12] Ramirez-Tortosa C, Andersen OM, Cabrita L, Gardner PT, Morrice PC, Wood SG, Duthie SJ, Collins AR and Duthie GG. Anthocyanin-rich extract decreases indices of lipid peroxidation and DNA damage in vitamin E-depleted rats. Free Radic Biol Med 2001; 31: 1033-1037.

[13] Zhou Z, Nan Y, Li X, Ma P, Du Y, Chen G, Ning N, Huang S, Gu Q, Li W and Yuan L. Hawthorn with "homology of medicine and food": a review of anticancer effects and mechanisms. Front Pharmacol 2024; 15: 1384189.

[14] Abou Baker DH. An ethnopharmacological review on the therapeutical properties of flavonoids and their mechanisms of actions: a comprehensive review based on up to date knowledge. Toxicol Rep 2022; 9: 445-469.

[15] Park MY, Kim Y, Ha SE, Kim HH, Bhosale PB, Abusaliya A, Jeong SH and Kim GS. Function and application of flavonoids in the breast cancer. Int J Mol Sci 2022; 23: 7732.

[16] Ofude M, Mizokami A, Kumaki M, Izumi K, Konaka H, Kadono Y, Kitagawa Y, Shin M, Zhang J, Keller ET and Namiki M. Repression of cell proliferation and androgen receptor activity in prostate cancer cells by 2'-hydroxyflavanone. Anticancer Res 2013; 33: 4453-4461.

[17] Nagaprashantha LD, Vatsyayan R, Singhal J, Lelsani P, Prokai L, Awasthi S and Singhal SS. 2'-hydroxyflavanone inhibits proliferation, tumor vascularization and promotes normal differentiation in VHL-mutant renal cell carcinoma. Carcinogenesis 2011; 32: 568-575.
[18] Yue Y, Qian W, Li J, Wu S, Zhang M, Wu Z, Ma Q and Wang Z. 2'-hydroxyflavanone inhibits the progression of pancreatic cancer cells and sensitizes the chemosensitivity of EGFR inhibitors via repressing STAT3 signaling. Cancer Lett 2020; 471: 135-146.
[19] Shin SY, Kim JH, Lee JH, Lim Y and Lee YH. 2'-Hydroxyflavanone induces apoptosis through Egr-1 involving expression of Bax, p21, and NAG-1 in colon cancer cells. Mol Nutr Food Res 2012; 56: 761-774.
[20] Wu S, Huang J, Hui K, Yue Y, Gu Y, Ning Z, Wang X, He D and Wu K. 2'-hydroxyflavanone inhibits epithelial-mesenchymal transition, and cell migration and invasion via suppression of the Wnt/beta-catenin signaling pathway in prostate cancer. Oncol Rep 2018; 40: 2836-2843.
[21] Wu K, Ning Z, Zhou J, Wang B, Fan J, Zhu J, Gao Y, Wang X, Hsieh JT and He D. 2'-hydroxyflavanone inhibits prostate tumor growth through inactivation of AKT/STAT3 signaling and induction of cell apoptosis. Oncol Rep 2014; 32: 131-138.
[22] Li Q, Wang H, Peng H, Huang Q, Huyan T, Huang Q, Yang H and Shi J. MicroRNAs: key players in bladder cancer. Mol Diagn Ther 2019; 23: 579-601.
[23] Shakeri A, Ghanbari M, Tasbandi A and Sahebkar A. Regulation of microRNA-21 expression by natural products in cancer. Phytother Res 2021; 35: 3732-3746.
[24] Zhang B, Tian L, Xie J, Chen G and Wang F. Targeting miRNAs by natural products: a new way for cancer therapy. Biomed Pharmacother 2020; 130: 110546.
[25] Liu Y, Li B, Yang X and Zhang C. MiR-99a-5p inhibits bladder cancer cell proliferation by directly targeting mammalian target of rapamycin and predicts patient survival. J Cell Biochem 2019; 120: 19330-19337.
[26] Shi Y, Bo Z, Pang G, Qu X, Bao W, Yang L and Ma Y. MiR-99a-5p regulates proliferation, migration and invasion abilities of human oral carcinoma cells by targeting NOX4. Neoplasma 2017; 64: 666-673.
[27] Inamoto T, Uehara H, Akao Y, Ibuki N, Komura K, Takahara K, Takai T, Uchimoto T, Saito K, Tanda N, Yoshikawa Y, Minami K, Hirano H, Nomi H, Kato R, Hayashi T and Azuma H. A panel of MicroRNA signature as a tool for predicting survival of patients with urothelial carcinoma of the bladder. Dis Markers 2018; 2018: 5468672.
[28] Du M, Shi D, Yuan L, Li P, Chu H, Qin C, Yin C, Zhang Z and Wang M. Circulating miR-497 and miR-663b in plasma are potential novel biomarkers for bladder cancer. Sci Rep 2015; 5: 10437.
[29] Lo UG, Pong RC, Yang D, Gandee L, Hernandez E, Dang A, Lin CJ, Santoyo J, Ma S, Sonavane R, Huang J, Tseng SF, Moro L, Arbini AA, Kapur P, Raj GV, He D, Lai CH, Lin H and Hsieh JT. IFN-gamma-induced IFIT5 promotes epithelial-to-mesenchymal transition in prostate cancer via miRNA processing. Cancer Res 2019; 79: 1098-1112.
[30] Huang J, Lo UG, Wu S, Wang B, Pong RC, Lai CH, Lin H, He D, Hsieh JT and Wu K. The roles and mechanism of IFIT5 in bladder cancer epithelial-mesenchymal transition and progression. Cell Death Dis 2019; 10: 437.
[31] Motzer RJ, Escudier B, Oudard S, Hutson TE, Porta C, Bracarda S, Grunwald V, Thompson JA, Figlin RA, Hollaender N, Urbanowitz G, Berg WJ, Kay A, Lebwohl D and Ravaud A; RECORD-1 Study Group. Efficacy of everolimus in advanced renal cell carcinoma: a double-blind, randomised, placebo-controlled phase III trial. Lancet 2008; 372: 449-456.
[32] Buti S, Leonetti A, Dallatomasina A and Bersanelli M. Everolimus in the management of metastatic renal cell carcinoma: an evidence-based review of its place in therapy. Core Evid 2016; 11: 23-36.
[33] Carmeliet P. VEGF as a key mediator of angiogenesis in cancer. Oncology 2005; 69 Suppl 3: 4-10.
[34] Martel RR, Klicius J and Galet S. Inhibition of the immune response by rapamycin, a new antifungal antibiotic. Can J Physiol Pharmacol 1977; 55: 48-51.
[35] Heitman J, Movva NR and Hall MN. Targets for cell cycle arrest by the immunosuppressant rapamycin in yeast. Science 1991; 253: 905-909.
[36] Miller TW, Balko JM and Arteaga CL. Phosphatidylinositol 3-kinase and antiestrogen resistance in breast cancer. J Clin Oncol 2011; 29: 4452-4461.
[37] du Rusquec P, Blonz C, Frenel JS and Campone M. Targeting the PI3K/Akt/mTOR pathway in estrogen-receptor positive HER2 negative advanced breast cancer. Ther Adv Med Oncol 2020; 12: 1758835920940939.
[38] Wang X, Yao Y and Gao J. Sevoflurane inhibits growth factor-induced angiogenesis through suppressing Rac1/paxillin/FAK and Ras/Akt/mTOR. Future Oncol 2020; 16: 1619-1627.
[39] Gong S, Hao X, Bi Y, Yang C, Wang W, Mickael HK, Zhang Y, Chen S, Qian Z, Huang F, Wei D and Yu W. Hepatitis E viral infection regulates estrogen signaling pathways: Inhibition of the

cAMPK-PKA-CREB and PI3K-AKT-mTOR signaling pathways. J Med Virol 2021; 93: 3769-3778.
[40] Wang X and Zhao XY. Transcription factors associated with IL-15 cytokine signaling during NK cell development. Front Immunol 2021; 12: 610789.
[41] Zhou J, Luo J, Wu K, Yun EJ, Kapur P, Pong RC, Du Y, Wang B, Authement C, Hernandez E, Yang J, Xiao G, Cha TL, Wu HC, Wu D, Margulis V, Lotan Y, Brugarolas J, He D and Hsieh JT. Loss of DAB2IP in RCC cells enhances their growth and resistance to mTOR-targeted therapies. Oncogene 2016; 35: 4663-4674.
[42] Lin JF, Tsai TF, Lin YC, Chen HE, Chou KY and Hwang TI. Benzyl isothiocyanate suppresses IGF1R, FGFR3 and mTOR expression by upregulation of miR-99a-5p in human bladder cancer cells. Int J Oncol 2019; 54: 2106-2116.
[43] Feng Y, Kang Y, He Y, Liu J, Liang B, Yang P and Yu Z. microRNA-99a acts as a tumor suppressor and is down-regulated in bladder cancer. BMC Urol 2014; 14: 50.
[44] Liu Y, Zhang K and Yang X. CircMCTP2 enhances the progression of bladder cancer by regulating the miR-99a-5p/FZD8 axis. J Egypt Natl Canc Inst 2024; 36: 8.
[45] Yoshimura A, Sawada K, Nakamura K, Kinose Y, Nakatsuka E, Kobayashi M, Miyamoto M, Ishida K, Matsumoto Y, Kodama M, Hashimoto K, Mabuchi S and Kimura T. Exosomal miR-99a-5p is elevated in sera of ovarian cancer patients and promotes cancer cell invasion by increasing fibronectin and vitronectin expression in neighboring peritoneal mesothelial cells. BMC Cancer 2018; 18: 1065.
[46] Tamai M, Tatarano S, Okamura S, Fukumoto W, Kawakami I, Osako Y, Sakaguchi T, Sugita S, Yonemori M, Yamada Y, Nakagawa M, Enokida H and Yoshino H. microRNA-99a-5p induces cellular senescence in gemcitabine-resistant bladder cancer by targeting SMARCD1. Mol Oncol 2022; 16: 1329-1346.

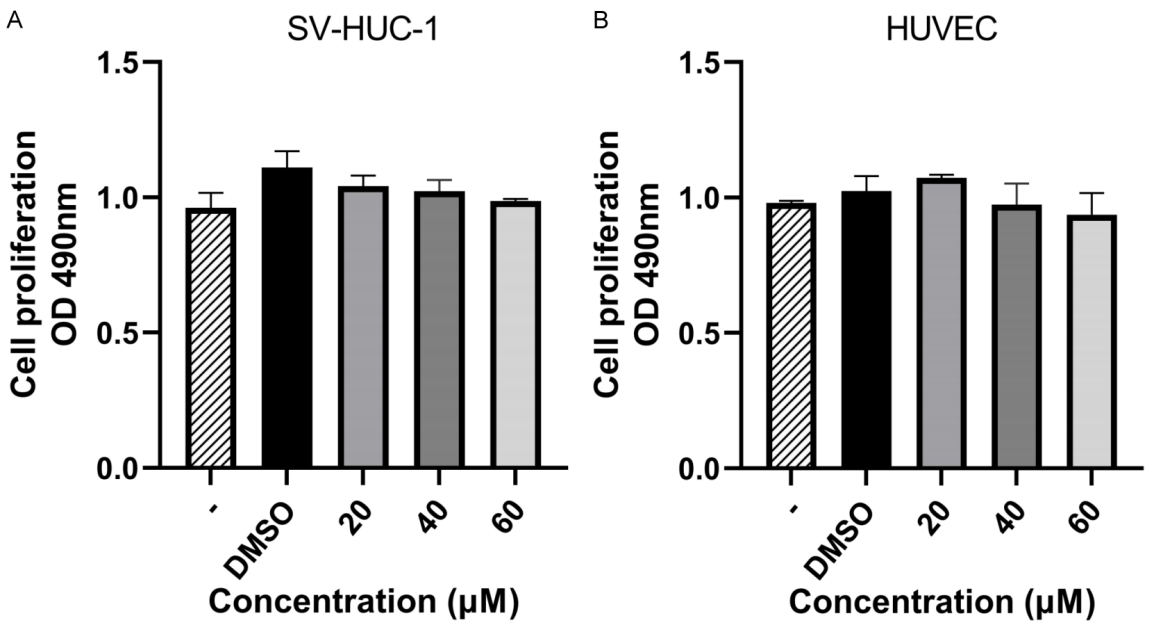

Figure S1. 2-HF has no significant effect on the activity and proliferation of normal bladder epithelial cells and vascular endothelial cells. A, B. MTT assay was used to measure the viability of SV-HUC-1 and HUVEC cells after 2HF treatment at 48 h.

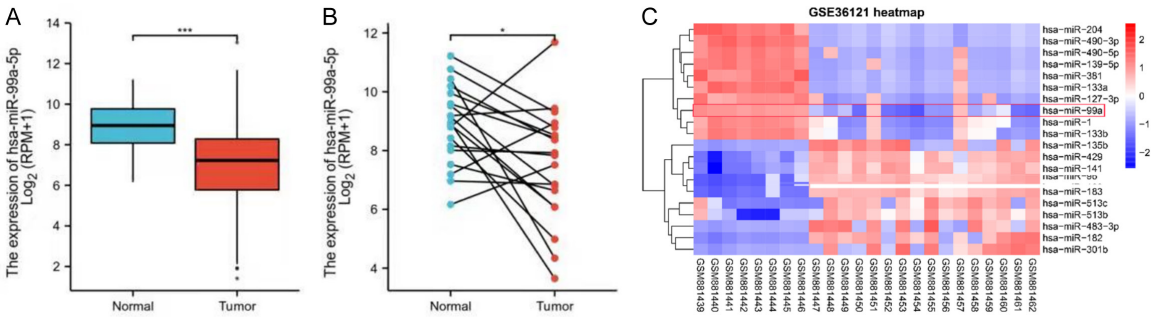

Figure S2. Expression of miR-99a-5p in BCa tissues. A, B. miR-99a-5p mRNA expression in normal bladder tissues and matched BCa tissues from TCGA database. C. Heat maps of key disordered miRNAs from GEO database (GSE36121).